A Section 508–conformant HTML version of this article is available at https://doi.org/10.1289/EHP4591.

Glucose Homeostasis following Diesel Exhaust Particulate Matter Exposure in a Lung Epithelial Cell-Specific IKK2-Deficient Mouse Model

Sufang Chen,[1,2] Minjie Chen,[2] Wei Wei,[2,3] Lianglin Qiu,[2,4] Li Zhang,[2] Qi Cao,[5] and Zhekang Ying[2]

[1]Department of Geriatric Endocrinology, First Affiliated Hospital of Zhengzhou University, Zhengzhou, China
[2]Department of Medicine Cardiology Division, University of Maryland School of Medicine, Baltimore, Maryland, USA
[3]Department of Bile Pancreatic Surgery, Xiangya Hospital, Central South University, Changsha, Hunan, China
[4]Department of Occupational and Environmental Health, School of Public Health, Nantong University, Nantong, China
[5]Department of Diagnostic Radiology and Nuclear Medicine, University of Maryland School of Medicine, Baltimore, Maryland, USA

Background: Pulmonary inflammation is believed to be central to the pathogenesis due to exposure to fine particulate matter with aerodynamic diameter ≤2.5 μm ($PM_{2.5}$). This central role, however, has not yet been systemically examined.

Objective: In the present study, we exploited a lung epithelial cell-specific inhibitor κB kinase 2 (IKK2) knockout mouse model to determine the role of pulmonary inflammation in the pathophysiology due to exposure to diesel exhaust particulate matter (DEP).

Methods: SFTPC-rtTA$^{+/-}$ tetO-cre$^{+/-}$ IKK2$^{flox/flox}$ (lung epithelial cell-specific IKK2 knockout, KO) and SFTPC-rtTA$^{+/-}$ tetO-cre$^{+/-}$ IKK2$^{flox/flox}$ (wild-type, tgWT) mice were intratracheally instilled with either vehicle or DEP for 4 months, and their inflammatory response and glucose homeostasis were then assessed.

Results: In comparison with tgWT mice, lung epithelial cell-specific IKK2-deficient mice had fewer DEP exposure-induced bronchoalveolar lavage fluid immune cells and proinflammatory cytokines as well as fewer DEP exposure-induced circulating proinflammatory cytokines. Glucose and insulin tolerance tests revealed that lung epithelial cell-specific IKK2 deficiency resulted in markedly less DEP exposure–induced insulin resistance and greater glucose tolerance. Akt phosphorylation analyses of insulin-responsive tissues showed that DEP exposure primarily targeted hepatic insulin sensitivity. Lung epithelial cell–specific IKK2-deficient mice had significantly lower hepatic insulin resistance than tgWT mice had. Furthermore, this difference in insulin resistance was accompanied by consistent differences in hepatic insulin receptor substrate 1 serine phosphorylation and inflammatory marker expression.

Discussion: Our findings suggest that in a tissue-specific knockout mouse model, an IKK2-dependent pulmonary inflammatory response was essential for the development of abnormal glucose homeostasis due to exposure to DEP. https://doi.org/10.1289/EHP4591

Introduction

Exposure to fine particulate matter with aerodynamic diameter ≤2.5 μm ($PM_{2.5}$) correlates with increased risk for type 2 diabetes mellitus and various abnormalities in glucose homeostasis (Bowe et al. 2018; Lucht et al. 2019; Lucht et al. 2018). However, how $PM_{2.5}$ exposure promotes the development of abnormal glucose homeostasis remains to be determined (EPA 2018). Putative mechanisms for this include: *a*) extrapulmonary translocation of $PM_{2.5}$ components; *b*) autonomic nervous system (ANS) dysfunction; and *c*) egress from the pulmonary inflammatory response (Rajagopalan et al. 2018). The evidence is strongest for egress from the pulmonary inflammatory response. Specifically, many studies have demonstrated that exposure to $PM_{2.5}$ causes pronounced pulmonary inflammation in humans (e.g., Habre et al. 2018; Kubesch et al. 2015) and in animal models (e.g., Happo et al. 2007; He et al. 2017), and a time course study revealed that $PM_{2.5}$ exposure-induced pulmonary inflammation preceded adverse extrapulmonary effects, such as systemic inflammation (Brook et al. 2010). As it is a consensus that systemic inflammation plays a crucial role in the pathogenesis of type 2 diabetes mellitus, pulmonary inflammation is postulated to be central to the pathogenesis of abnormal glucose homeostasis due to exposure to $PM_{2.5}$ (Brook et al. 2017). Consistent with this notion, we recently showed that pulmonary inflammation subsequent to lung epithelial cell-specific overexpression of constitutively active inhibitor κB kinase 2 (IKK2ca) was sufficient to induce marked insulin resistance (Chen et al. 2017). However, we also found that 5 wk of withdrawal from exposure to $PM_{2.5}$ resolved $PM_{2.5}$ exposure–induced extrapulmonary inflammation, vascular dysfunction, and hypertension, but not pulmonary inflammation (Ying et al. 2015), suggesting that a mechanism other than pulmonary inflammation may also be involved in $PM_{2.5}$ exposure–induced systemic inflammation or abnormalities in glucose homeostasis. Further studies are thus needed to pinpoint the role of pulmonary inflammation in the development of adverse effects due to $PM_{2.5}$ exposure.

IKK2 regulates nuclear factor-kappaB (NF-κB) activity and plays a crucial role in both acute and chronic inflammations (Pahl 1999). Studies have shown that exposure to $PM_{2.5}$ activates the IKK2/NF-κB pathway in various tissues, including the lung (Dagher et al. 2007; Kafoury and Madden 2005; Maciejczyk and Chen 2005; Mantecca et al. 2010; Nam et al. 2004). Furthermore, inhibition of IKK2 blocked $PM_{2.5}$ exposure–induced expression of inflammatory cytokines in respiratory epithelial cells (Li et al. 2013) and alveolar macrophages (Kafoury and Madden 2005), suggesting that targeting pulmonary IKK2 might disconnect $PM_{2.5}$ exposure and pulmonary inflammation. In the present study, we therefore generated lung epithelial cell–specific IKK2-deficient mice (SFTPC-rtTA$^{+/-}$ tetO-cre$^{+/-}$ IKK2$^{flox/flox}$) and used them to ascertain the role of pulmonary inflammation in the pathogenesis of insulin resistance due to exposure to diesel exhaust particulate matter (DEP).

Materials and Methods

Animals

University of Maryland, Baltimore (UMB) is an AAALAC-accredited institution. All procedures in this study were approved by the Institutional Animal Care and Use Committee (IACUC) at

Address correspondence to Zhekang Ying, 20 Penn St. HSFII S022, Baltimore, MD 21201, USA, Telephone: 410-328-2063; Fax: 410-328-1048. Email: Yingzhekang@hotmail.com or Zying@medicine.umaryland.edu

The authors declare they have no actual or potential competing financial interests.

Received 13 October 2018; Revised 25 April 2019; Accepted 26 April 2019; Published 16 May 2019.

UMB, and all the animals were treated humanely and with regard for alleviation of suffering. SFTPC-rtTA (Stock No. 016146) and tetO-cre (Stock No. 006224) transgenic mice were obtained from Jackson Laboratories. The generation of $IKK2^{flox/flox}$ mice were previously described (Maeda et al. 2003). Male SFTPC-$rtTA^{+/-}$ tetO-$cre^{+/-}$ $IKK2^{flox/flox}$ (3 for Figure 1B, 5 for Figures 1C and 1D, 6 for instillation of PBS, and 7 for instillation of DEP) and male SFTPC-$rtTA^{+/-}$ tetO-$cre^{-/-}$ $IKK2^{flox/flox}$ littermates (3 for Figure 1B, 5 for Figures 1C and 1D, 7 for instillation of PBS, and 8 for instillation of DEP) were generated through crossing between SFTPC-$rtTA^{+/+}$ tetO-$cre^{+/-}$ $IKK2^{flox/flox}$ and $IKK2^{flox/flox}$. To induce the deletion of IKK2, after weaning, all the mice were fed with doxycycline in their diet (625 mg/kg diet, Envigo TD.01306) for 8 wk. Due to the concern about the doxycycline feeding as a potential confounding factor, all the mice in this study were not fed with the doxycycline diet beyond the 8 wk of doxycycline feeding. To prevent confusion, in the present study, these doxycycline diet–fed male SFTPC-$rtTA^{+/-}$ tetO-$cre^{+/-}$ $IKK2^{flox/flox}$ mice and male SFTPC-$rtTA^{+/-}$ tetO-$cre^{-/-}$ $IKK2^{flox/flox}$ littermates are referred to as knockout (KO) and wildtype (tgWT) mice, respectively. All the mice were housed in standard cages (Super Mouse 1800™ Ventilated Racks & Cages; Lab Products, Inc.) with full access to diet [either the doxycycline diet or Teklad global 14% protein (Envigo) diet, replaced weekly] and water (replaced weekly). The room was kept with a 12-h light/12-h dark cycle, temperatures of 65 to 75°F, and 40 to 60% humidity. The mice used in the present study were weaned when 21–24 days old.

PCR Genotyping and Confirming the Deletion of IKK2 by the Doxycycline Feeding

All one-week-old newborns were subjected to tail biopsying, and the genomic DNA were extracted from those biopsies. The genotype of each mouse was determined by polymerase chain reaction (PCR), using the genotyping primers (Table 1). The PCR cycling parameters included: 4 min predenaturing at 94°C and 35 cycles of 30-s denaturing at 94°C, 30-s annealing at 60°C, and 60-s extension at 72°C. Before PBS/DEP instillation, all the mice were genotyped again as described above to verify their genotypes. To confirm the induced deletion of IKK2 by the doxycycline feeding, three tgWT and three KO were euthanized at the end of the doxycycline feeding, and the genomic DNA were extracted from the heart, liver, lung, and kidney. The WT, floxed, and Δ alleles were visualized by PCR using the deletion-confirming primers in Table 1 (obtained from Sigma-Aldrich). The above-mentioned PCR cycling parameters were applied.

DEP Intratracheal Instillation

DEP was obtained from the National Institute of Standards and Technology (DEP, NIST® SRM® 2975). The chemical characterization of this DEP is available at www-s.nist.gov/srmors/certificates/2975.pdf. Its mean diameter of particles was 1.62 ± 0.01 μm. It was stored at 4°C and kept away from direct sunlight. To perform instillation, DEP was suspended in sterile phosphate-buffered saline (PBS). To minimize aggregation, DEP suspensions were sonicated (Clifton Ultrasonic Bath) for 20 min on the day of instillation and vortexed 30 s before each instillation. The instillation of DEP was initiated when mice were 12–14 wk old (1–2 wk after 8-wk feeding of the doxycycline diet). The KO and tgWT mice were housed mixedly, and each cage was randomly allocated to either PBS or DEP instillation. The instillation of DEP was performed as previously described (Kyjovska et al. 2015), with minor modifications. Briefly, to instill DEP, the animals were anesthetized with 3% isoflurane and placed supine with extended necks on an angled board. A Becton Dickinson 18 Gauge cannula was inserted via the mouth into the trachea. DEP suspension (20 μg in 50 μl, approximately equating to inhalational exposure to 160 $\mu g/m^3$ $PM_{2.5}$) (Bide et al. 1997) or PBS (50 μl) were intratracheally instilled via a sterile syringe and followed by an air bolus of 150 μl. The intubation catheter was removed and the mouse transferred to a vertical hanging position with the head up for 5 min, ensuring that the delivered material was maintained in the lung and did not block the airways. Either DEP or PBS was instilled 3 times per week (Monday, Wednesday, and Friday) for 19 wk.

Intraperitoneal Glucose Tolerance Test (IPGTT) and Glucose-Induced Insulin Secretion Assessment

IPGTT was performed monthly (on the fourth Tuesday of each month) during the 4-month exposure to DEP. Before testing, mice were fasted for 16 h. The blood of mouse tail vein was collected through a small cut to determine the blood glucose level. On the day of the experiments, after determination of basal (0 min) blood glucose level using an automatic glucometer (Glucotrend 2, Roche Diagnostics), mice were intraperitoneally injected with glucose [2 g/kg body weight (BW)]. Blood glucose levels at 15, 30, 60, and 120 min after injection of glucose were then measured using the automatic glucometer. When performing the last IPGTT (4-month exposure), sera at 0, 15, and 30 min were harvested, and their insulin levels were determined using Ultra Sensitive Mouse Insulin ELISA Kit (Crystal Chem, Inc.) per the manufacturer's instructions. To harvest the sera, the blood of mouse tail vein was allowed to clot for 30 min at room temperature, and then centrifuged at 10,000 rpm and 4°C for 10 min. The supernatants were transferred to new tubes and kept at −80°C until the assessment of insulin.

Insulin Tolerance Test (ITT)

ITT was performed (one week after the last IPGTT) after the 4-month exposure to DEP. Before testing, mice were fasted for 4 h. The blood of mouse tail vein was collected through a small cut for determining the blood glucose level. After determination of basal blood glucose level using an automatic glucometer (Glucotrend 2), mice were intraperitoneally injected with insulin (0.5 U/kg BW). Blood glucose levels at 15, 30, 60, and 120 min after injection of insulin were then measured as described above.

Animal Euthanasia, Bronchoalveolar Lavage, and Tissue Harvesting

Animals were fasted overnight and injected intraperitoneally with insulin (10 U/kg BW). This high dose of insulin is generally used for assessing insulin-induced Akt phosphorylation in the insulin-responsive tissues (Kim et al. 1999, 2000). After 20 min, animals were euthanized by overdose of isoflurane. Blood was collected from the heart and centrifuged at 3,000 rpm for 5 min. Plasma and all other tissues (liver, epididymal adipose tissue, and skeletal muscle) were immediately stored first in dry ice and then at −80°C until further processing.

To perform bronchoalveolar lavage, the mouse lung, trachea, and heart were removed and put on ice. Through a tracheal cannula, 1 mL sterile PBS with 0.1 mM ethylenediaminetetraacetic acid (EDTA) was instilled and withdrawn to recover bronchoalveolar lavage fluid (BALF). This lavage was performed three times in total. The total number of cells in the collected BALF (around 3 mL) was estimated using a hemocytometer. After 5 min centrifuge at 1,500 rpm, the BALF were stored in dry ice and then −80°C until further processing, and the precipitated cells were used for BALF cell differentiation. Cytospin slides were prepared using Shandon Cytospin 3™ (Thermo Scientific) and stained

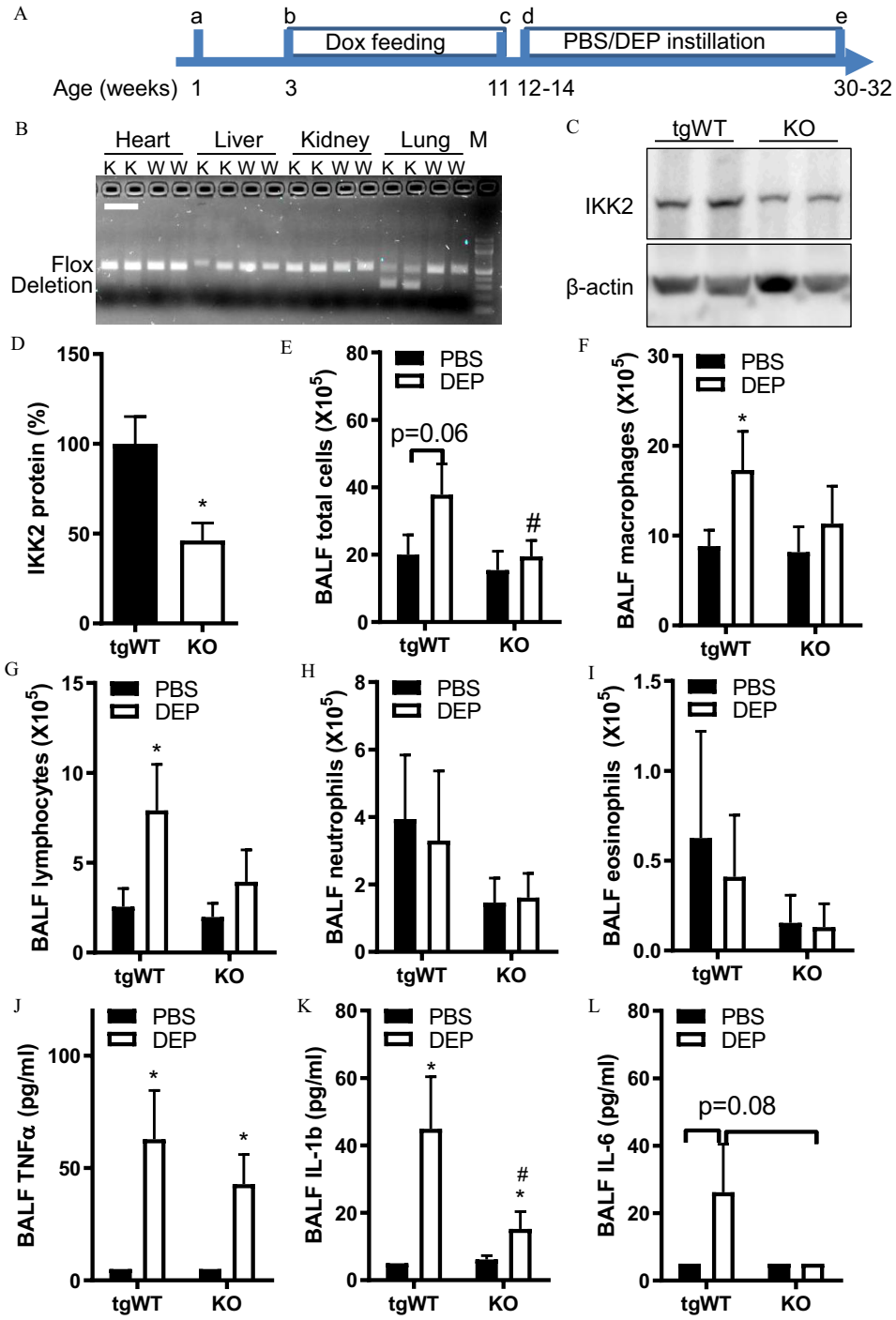

Figure 1. Pulmonary inflammation after diesel exhaust particulate matter (DEP) treatment in mice with lung epithelial cell-specific IKK2 deficiency. (A) The experimental scheme. a, genotyping; b, weaning and initiation of doxycycline (Dox) feeding; c, assessments of induced knockout by PCR and Western blotting; d, initiation of phosphate buffered saline (PBS)/DEP instillation; e, euthanizing and tissue-harvesting. (B) SFTPC-rtTA$^{+/-}$ tetO-cre$^{+/-}$ IKK2$^{flox/flox}$ (knockout, KO) and littermate control (SFTPC-rtTA$^{+/-}$ tetO-cre$^{-/-}$ IKK2$^{flox/flox}$, transgenic wild-type control, tgWT) were fed with a doxycycline diet (625 mg/kg diet) for 8 wk. Subgroups of these mice were immediately euthanized, the indicated tissues were isolated and their deletion of IKK2 was assessed by PCR. A representative result is presented. Of all those tested mice ($n = 3$/group), no evident outlier in any group was noted. K, KO; W, tgWT. The scale marker equals 1 cm. (C and D) KO and littermate control (tgWT) were euthanized immediately after the 8-wk feeding with a doxycycline diet (625 mg/kg diet), and their lungs were isolated and subjected to Western blotting analysis of IKK2 protein expression. A representative image (C) and quantitation of results as a percentage of the β-actin loading control (D) are presented. $n = 5$/group. $^{*}p < 0.05$ vs. tgWT, Student's t test. (E–L) KO and tgWT mice were subjected to a 4-month intratracheal instillation of either PBS or DEP. After euthanasia, BALF cells were differentiated (E–I). Levels of the indicated cytokines in those BALFs were assessed using the BD Cytometric Bead Array Kit (J–L). $n = 6$–8/group. All data were expressed as means ± SEMs. $^{*}p < 0.05$ vs. PBS, $^{\#}p < 0.05$ vs. tgWT, two-way ANOVA followed by Bonferroni correction.

Table 1. Primer sequences for RT-PCR.

	Forward primer	Reverse primer
F4/80	TGTCTGACAATTGGGATCTGCCCT	TTGCATGTTCAGGGCAAACGTCTC
GAPDH	GCAGTGGCAAAGTGGAGATTGTTGC	CCCGTTGATGACAAGCTTCCCATTC
IL-6	ATCCAGTTGCCTTCTTGGGACTGA	TAAGCCTCCGACTTGTGAAGTGGT
TNFα	TTCCGAATTCACTGGAGCCTCGAA	TGCACCTCAGGGAAGAATCTGGAA
IL-1β	ACGGACCCCAAAAGATGAAG	TTCTCCACAGCCACAATGAG
MCP1	GCTCAGCCAGATGCAGTTAA	TCTTGAGCTTGGTGACAAAAACT
IKK2 deletion-confirming[a]	CGCCTAGGTAAGATGGCTGTCT	Primer 1: GTGGTCATAGGTCTGGTTGTCC Primer 2: TAGTCCAACTGGCAGCGAATAC
IKK2 genotyping[b]	GTCATTTCCACAGCCCTGTGA	CCTTGTCCTATAGAAGCACAAC
SFTPC-rtTA genotyping	CGCTGTGGGGCATTTTACTTTAG	CATGTCCAGATCGAAATCGTC
Cre genotyping	ACCTGATGGACATGTTCAGGGATCG	TCCGGTTATTCAACTTGCACCATGC

[a]To confirm the deletion of IKK2 by the treatment with doxycycline, three primers were used and visualized all three alleles (WT, floxed, and recombinant [Δ]) in one PCR reaction.
[b]To genotype the IKK2 gene, two primers were used and visualized the WT and floxed alleles only.

with Diff-Quik solution (EMS) per the manufacturers' protocols. Differential cell counts for neutrophils, eosinophils, macrophages, monocytes, and lymphocytes were assessed by a pathologist who was blinded to the grouping.

Plasma and BALF cytokine analysis. Plasma and BALF cytokine levels were assessed using the flex set of BD™ Cytometric Bead Array Kit (BD Biosciences, Catalog No. 560232, 558301, and 558299) per the manufacturer's instructions. We assessed these three cytokines because they are the most frequently used markers for evaluating the inflammatory level. Briefly, 25 μL per mouse plasma were incubated with the beads, and the signaling was assessed by BD Canto II flow cytometry per the manual of the BD™ Cytometric Bead Array Kit. The TNFα, interleukin (IL)-1β (IL-1β, and IL-6 levels of each sample were then determined using the standard curves. To facilitate statistical analysis, the cytokine level of all samples measuring below the detection limit (provided by the manufacturer) was imputed to be the detection limit itself.

Western Blotting

Lysates of liver, epididymal adipose tissue, and skeletal muscle were prepared using radioimmunoprecipitation assay (RIPA) buffer (MilliporeSigma) supplemented with protease and phosphatase inhibitors (Sigma, Catalog No. P2714 and P5726). Briefly, for each sample, a ~5 mg piece of tissue was cut on ice. Next, ~300 μL of ice-cold lysis buffer was added rapidly to the tube. The tissues were homogenized with Bead Ruptor Elite Bead Mill Homogenizer (OMNI International) for 5 min, then maintained with constant agitation for 30 min at 4°C. These lysates were then centrifuged for 20 min at 12,000 rpm at 4°C. The supernatants were transferred to fresh tubes on ice. The protein level for each sample was determined using Pierce™ BCA Protein Assay Kit (ThermoFisher). For each sample, 40 μg protein was then separated by 10% SDS-polyacrylamide gel electrophoresis [freshly prepared using the PROTEAN® II XL Cell system (Bio-Rad)] and electroblotted onto polyvinylidene fluoride membranes (Immun-Blot PVDF Membrane; Bio-Rad, Catalog No. 1620177). The membrane was blocked using Amersham ECL Prime Blocking Reagent (Catalog No. RPN418) for 1 h at room temperature and then incubated with each of the following primary antibodies overnight at 4°C: 1:500 diluted Phospho-IRS-1 (Ser307) Antibody #2381 (Cell Signaling Technology), 1:500 diluted Phospho-IRS-1 (Ser1101) Antibody #2385 (Cell Signaling Technology), 1:1,000 diluted IRS-1 Antibody #3194 (Cell Signaling Technology), 1:500 diluted Phospho-SAPK/JNK (Thr183/Tyr185) (G9) Mouse mAb #9255 (Cell Signaling Technology), 1:1,000 diluted SAPK/JNK Antibody #9252 (Cell Signaling Technology), 1:500 diluted Phospho-IKKα/β (Ser176/180) Antibody II #2694 (Cell Signaling Technology), 1:1,000 diluted IKKβ (D30C6) Rabbit mAb #8943 (Cell Signaling Technology), and 1:10,000 diluted Monoclonal Anti-β-Actin Antibody A5316 (Sigma-Aldrich). After washing with TBST buffer 3 times (10 min per time), the membrane was incubated with 1:5,000 diluted secondary antibodies conjugated with horseradish peroxidase (Amersham, Catalog Nos. NA931-1ML and NA934-1ML) for 1 h at room temperature. After washing with TBST buffer 3 times (10 min per time), the target proteins were visualized with the chemiluminescence reagent (Amersham, Catalog No. RPN2232). The images were acquired using ImageQuant LAS 4000 (Amersham) per the manufacturer's instructions. Densities of target protein bands were determined with Quantity One® 1-D 4.4.1 Software (Bio-Rad).

Quantitative Reverse Transcriptase Polymerase Chain Reaction (RT-PCR)

Total RNA was isolated from the livers with Invitrogen™ TRIzol™ reagent (Invitrogen) per the manufacturer's instructions. The RNA concentrations were determined using NanoDrop™ 2000/2000c Spectrophotometers (Thermo Fisher). Any sample with an OD260/OD280 ratio below 1.2 was not used. In addition, 2 μg total RNA was reverse-transcribed using random hexamers and the ThermoScript™ RT-PCR System (Invitrogen). Quantitative real-time polymerase chain reaction (RT-PCR) was performed with a LightCycler® 480 Instrument II (Roche) and SYBER Green PCR Master Mix (Applied Biosystems). The sequences of primers are presented in Table 1 and obtained from Sigma-Aldrich. The relative expression level was obtained as described previously (Ying et al. 2009). Briefly, Ct values were acquainted using the built-in software of LightCycler® 480 Instrument II, and differences of Ct value between target gene and GAPDH (ΔCt) and then $2^{\Delta Ct}$ were calculated.

Statistics

All data are expressed as means ± Standard Error of the Means (SEMs) unless noted otherwise. Statistical tests were performed using one-way or two-way analysis of variance (ANOVA) followed by Bonferroni correction or unpaired *t*-test using GraphPad Prism (version 5; GraphPad Software). The significance level was set at $p < 0.05$.

Results

Pulmonary Inflammation after DEP Treatment in Mice with Lung Epithelial Cell-Specific IKK2 Deficiency

To ascertain the role of pulmonary inflammation in $PM_{2.5}$ exposure–induced pathogenesis, we generated SFTPC-rtTA$^{+/-}$ tetO-cre$^{+/-}$ IKK2$^{flox/flox}$ and littermate control (SFTPC-rtTA$^{+/-}$ tetO-cre$^{-/-}$ IKK2$^{flox/flox}$) mice. PCR analysis showed that the 8-

wk feeding with doxycycline diet resulted in marked IKK2 gene recombination in the lung, but not in the heart, liver, or kidney (Figure 1B). This recombination of IKK2 gene in the lung was concurrent with significantly lower expression of pulmonary IKK2 protein (Figures 1C and D).

To determine the effect of lung epithelial cell–specific IKK2 deficiency on $PM_{2.5}$-exposure–induced pulmonary inflammation, doxycycline diet–fed male SFTPC-rtTA$^{+/-}$ tetO-cre$^{+/-}$ IKK2$^{flox/flox}$ (KO) and SFTPC-rtTA$^{+/-}$ tetO-cre$^{-/-}$ IKK2$^{flox/flox}$ littermates (tgWT) were subjected to 4-month intratracheal instillation of DEP or PBS. BALF cell counting revealed that DEP-instilled tgWT mice vs. PBS-instilled tgWT mice, but not DEP-instilled KO mice vs. PBS-instilled KO mice, had greater BALF total cell numbers (Figure 1E), a frequently used indicator of pulmonary inflammation. BALF cell differentiation showed that DEP-instilled tgWT mice vs. PBS-instilled tgWT mice, but not DEP-instilled KO mice vs. PBS-instilled KO mice, had higher macrophages and lymphocytes in BALF (Figures 1F–1G). BALF proinflammatory cytokine levels are also frequently used as indicators of pulmonary inflammation. BALF proinflammatory cytokine assessments showed that DEP-instilled tgWT mice had higher levels of BALF tumor necrosis factor α (TNFα), IL-1β, and IL-6 than those of PBS-instilled tgWT mice (Figures 1J–1L). The differences in the BALF proinflammatory cytokine levels between DEP-instilled and PBS-instilled KO mice were smaller than those between DEP-instilled and PBS-instilled tgWT mice (Figures 1J–1L).

Levels of Circulating Proinflammatory Cytokines after DEP Treatment in Mice with Lung Epithelial Cell–Specific IKK2 Deficiency

We also assessed the levels of circulating proinflammatory cytokines. The assessments of circulating proinflammatory cytokines showed that DEP-instilled tgWT mice had higher levels of circulating TNFα and IL-6 than levels in PBS-instilled tgWT mice, whereas DEP-instilled KO mice had almost comparable levels of circulating TNFα and IL-6 in comparison with levels in PBS-instilled KO mice (Figure 2).

Glucose Metabolism in DEP-Exposed Mice with Lung Epithelial Cell–Specific IKK2 Deficiency

To ascertain the time dependency of glucose metabolic effect of DEP exposure, IPGTT was performed monthly on these DEP- or vehicle-treated mice. The results of IPGTT revealed that after 3-month and 4-month exposures, DEP-exposed tgWT mice had significantly lower glucose tolerance in comparison with that of PBS-exposed tgWT mice, whereas DEP-exposed KO mice had almost comparable glucose tolerance in comparison with that of PBS-exposed KO mice (Figures 3A–3H). Furthermore, ITT showed that, after the 4-month exposure, DEP-exposed tgWT mice had significantly higher glucose-induced insulin secretion in comparison with glucose-induced insulin secretion in PBS-exposed tgWT mice (Figures 3I and 3J) and lower systemic insulin sensitivity (Figures 3K and 3L). Coincident with the above-mentioned inflammation analyses, DEP-exposed KO mice had markedly smaller differences in glucose-induced insulin secretion in comparison with glucose-induced insulin secretion of PBS-exposed KO mice (Figures 3I and 3J) and almost comparable sensitivity to insulin (Figures 3K and 3L).

Insulin Tolerance in DEP-Exposed Mice with Lung Epithelial Cell–Specific IKK2 Deficiency

To further document the mechanism whereby DEP exposure results in systemic insulin resistance, we assessed Akt phosphorylation level, a reflection of local insulin signaling (Guo 2014), in insulin-sensitive tissues, including the liver, adipose tissue, and skeletal muscle. DEP-exposed tgWT mice had significantly lower insulin-induced Akt phosphorylation in the liver in comparison with that of PBS-exposed tgWT mice (Figures 4A and 4B), but DEP-exposed tgWT mice and PBS-exposed tgWT mice had comparable insulin-induced Akt phosphorylation in the adipose tissue and skeletal muscle (Figures 4A and 4B), suggesting that DEP exposure induces glucose intolerance primarily through induction of hepatic insulin resistance. Consistent with the investigation of systemic insulin resistance (Figure 3), DEP-exposed KO mice and PBS-exposed KO mice had comparable Akt phosphorylation in the liver, adipose tissue, and skeleton muscle (Figures 4A and 4B).

Hepatic IRS-1 Phosphorylation and Inflammatory Response in DEP-Exposed Mice with Lung-Specific IKK2 Deficiency

In line with the assessment of hepatic insulin signaling (Figure 4), DEP-instilled tgWT mice had higher hepatic IRS-1 Ser307 and Ser1101 phosphorylation levels in comparison with levels in PBS-instilled tgWT mice, whereas DEP-instilled KO mice and PBS-instilled KO mice had comparable hepatic IRS-1 serine phosphorylation (Figures 5A and 5B). To determine whether a local inflammatory response mediates DEP exposure inducing hepatic insulin resistance, we assessed hepatic activities of IKK2 and c-Jun NH_2-terminal kinase (JNK), two central regulators of

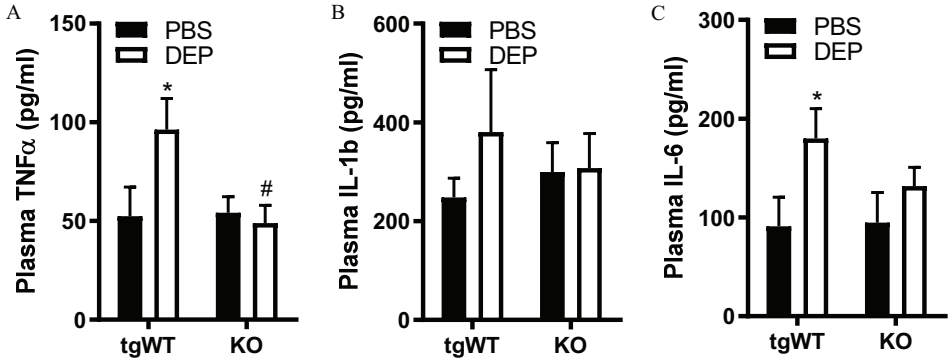

Figure 2. Levels of circulating pro-inflammatory cytokines after diesel exhaust particulate matter (DEP) treatment in mice with lung epithelial cell-specific IKK2 deficiency. Plasma were harvested after phosphate buffered saline (PBS) or DEP-treated mice were euthanized and levels of TNFα (A), interleukin-1β (IL-1β) (B), and IL-6 (C) were determined using the BD Cytometric Bead Array Kit. $n = 6–8$/group. All data were expressed as means ± SEMs. $^{*}p < 0.05$ vs. PBS, $^{\#}p < 0.05$ vs. tgWT, two-way ANOVA followed by Bonferroni correction. KO, SFTPC-rtTA$^{+/-}$ tetO-cre$^{+/-}$ IKK2$^{flox/flox}$ mice; tgWT, SFTPC-rtTA$^{+/-}$ tetO-cre$^{-/-}$ IKK2$^{flox/flox}$ littermates.

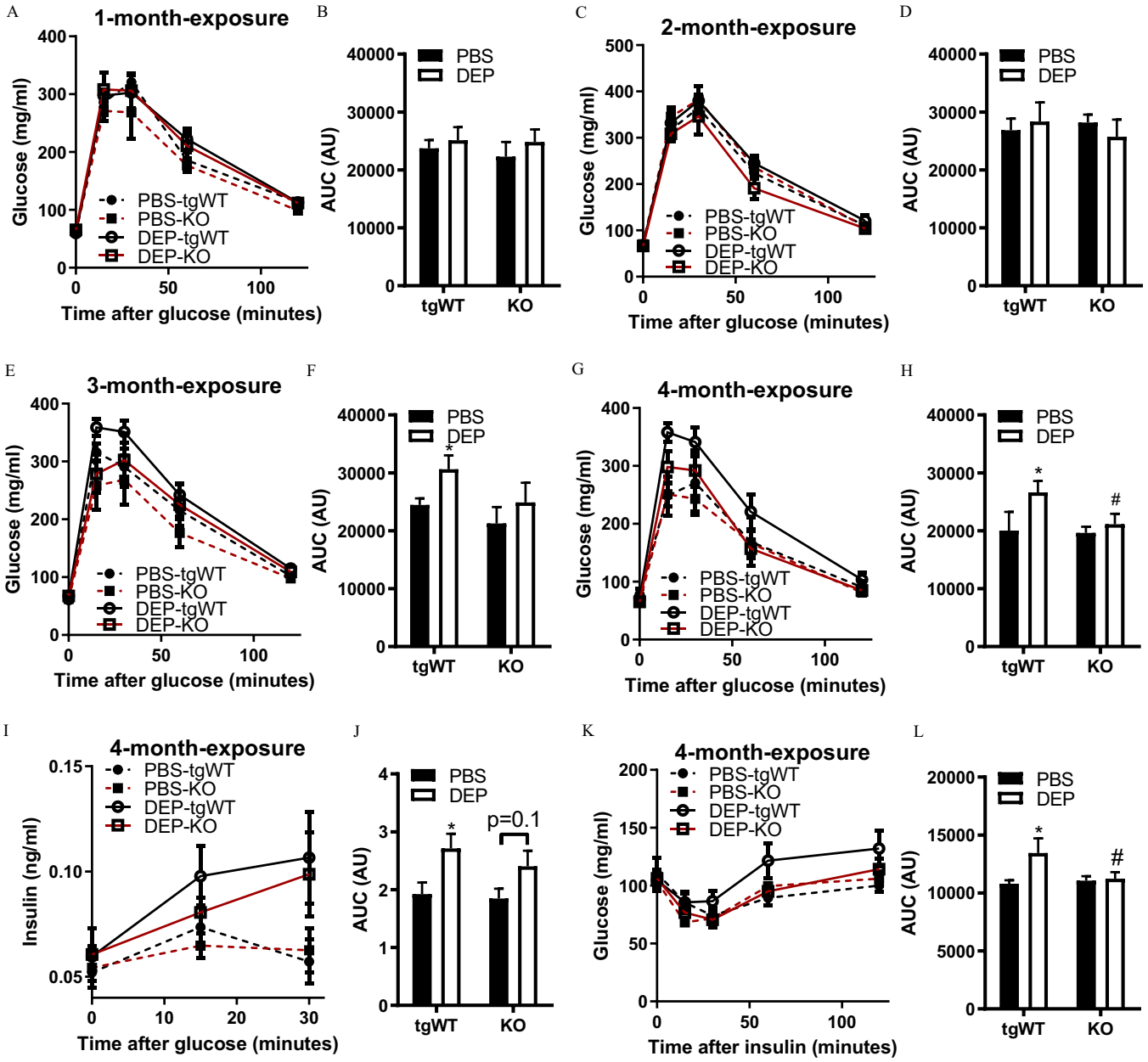

Figure 3. Glucose metabolism in diesel exhaust particulate matter (DEP)-exposed mice with lung epithelial cell-specific IKK2 deficiency. (A–H) Intraperitoneal glucose tolerance test (IPGTT) was performed monthly when KO and tgWT mice were being subjected to phosphate buffered saline (PBS) or DEP instillation. Both the response curves (A, C, E, and G) and summarization of area under the curve (AUC, B, D, F, and H) are presented. (I and J) When performing the last IPGTT (4-month instillation), sera were collected at the indicated timepoints, and their insulin levels were determined. The response curves (I) and summarization of AUC (J) are presented. (K and L) Insulin tolerance test (ITT) was performed 1 wk after the last IPGTT. The response curves (K) and summarization of AUC (L) are presented. $n = 6–8$/group. All data were expressed as means ± SEMs. $*p < 0.05$ vs. PBS, $^{\#}p < 0.05$ vs. tgWT, two-way ANOVA followed by Bonferroni correction. KO, SFTPC-rtTA$^{+/-}$ tetO-cre$^{+/-}$ IKK2$^{flox/flox}$ mice; tgWT, SFTPC-rtTA$^{+/-}$ tetO-cre$^{-/-}$ IKK2$^{flox/flox}$ littermates.

the inflammatory response. Our results revealed that DEP-instilled tgWT mice had significantly higher phosphorylation levels of IKK2 and JNK in comparison with those levels in PBS-instilled tgWT mice (Figures 5C and 5D), suggesting that both hepatic IKK2 and JNK signaling pathways are activated by exposure to DEP. Furthermore, we found that DEP-instilled KO mice and PBS-instilled KO mice had comparable hepatic IKK2 and JNK phosphorylation levels. Consistent with the analyses of IKK2 and JNK activity, quantitative PCR analyses revealed that DEP-instilled tgWT mice had significantly higher hepatic mRNA expression levels of TNFα, IL-1β, IL-6, monocyte chemoattractant protein 1 (MCP-1), and the mouse macrophage marker F4/80 than expression levels found in PBS-instilled tgWT, whereas DEP-instilled KO mice and PBS-instilled KO had comparable IL-1β and IL-6 mRNA expression (Figure 6); additionally, the differences in the expression levels of TNFα, MCP-1, and F4/80 were also markedly lower than those between DEP-instilled tgWT mice and PBS-instilled tgWT mice (Figure 6).

Discussion

Compelling evidence has demonstrated that exposure to $PM_{2.5}$ correlates with various abnormalities in glucose homeostasis and increased risk for type 2 diabetes mellitus (Bowe et al. 2018;

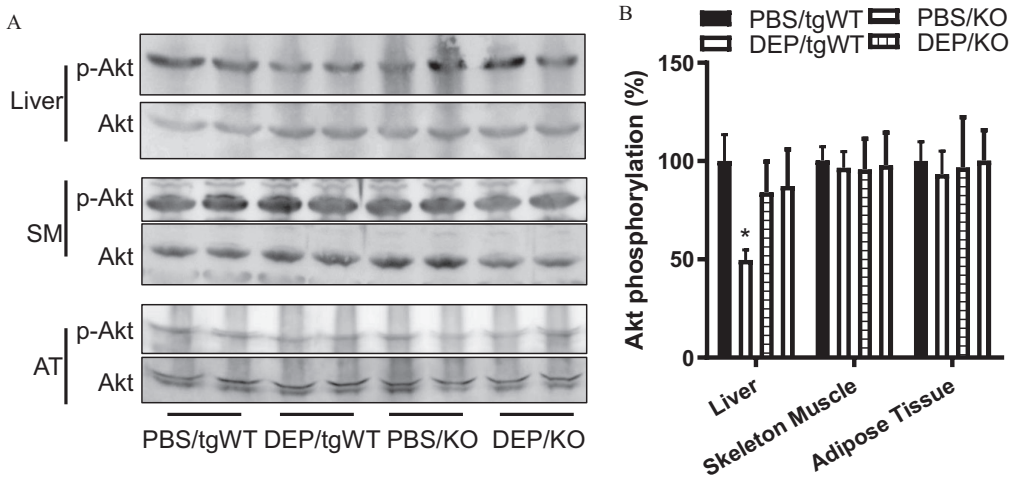

Figure 4. Insulin sensitivity in diesel exhaust particulate matter (DEP)-exposed mice with lung epithelial cell-specific IKK2 deficiency. Before euthanasia, those phosphate buffered saline (PBS) or DEP-treated mice were injected intraperitoneally with insulin (10 U/kg body weight), and the insulin-responsive tissues, including liver, epididymal adipose tissue (AT), and skeleton muscle (SM), were isolated and subjected to western blot analysis of Akt phosphorylation. Representative images (A) and quantitation data (B) are presented. To quantitate the phosphorylation, the phosphor-Akt level was normalized to total Akt and graphed in relation to PBS/tgWT. $n = 6–8$/group. All data were expressed as means ± SEMs. $*p < 0.05$ vs. PBS, two-way ANOVA followed by Bonferroni correction. KO, SFTPC-rtTA$^{+/-}$ tetO-cre$^{+/-}$ IKK2$^{flox/flox}$ mice; tgWT, SFTPC-rtTA$^{+/-}$ tetO-cre$^{-/-}$ IKK2$^{flox/flox}$ littermates.

Lucht et al. 2019, 2018). Pulmonary inflammation is believed to be central to the development of adverse health effects due to exposure to $PM_{2.5}$ (Rajagopalan et al. 2018), such as abnormal glucose homeostasis. This role of pulmonary inflammation, however, had not yet been systemically investigated. To ascertain the role of pulmonary inflammation in the pathogenesis due to exposure to $PM_{2.5}$, the present study used SPFTC-rtTA and tetO-cre alleles to knock out IKK2 specifically in lung epithelial cells, and assessed how this genetic manipulation affected DEP exposure–induced pulmonary inflammation and abnormalities in glucose homeostasis. The major findings in this study suggest that: *a*) lung epithelial cell-specific IKK2 deficiency was sufficient to reduce DEP exposure-induced pulmonary inflammation; *b*) lung epithelial cell–specific IKK2 deficiency nearly abolished DEP exposure–induced systemic insulin resistance and subsequent glucose intolerance; *c*) DEP exposure caused glucose intolerance primarily through induction of hepatic insulin resistance, paralleled by higher hepatic IRS-1 serine phosphorylation and expression of inflammatory markers; and *d*) lung epithelial cell–specific IKK2 deficiency ameliorated DEP exposure–induced hepatic inflammation and insulin resistance. Collectively, our data, which was generated in a transgenic mouse model, indicate that pulmonary inflammation is essential for the pathogenesis of abnormal glucose homeostasis due to exposure to DEP.

The lung is the primary target organ of inhaled $PM_{2.5}$, and pulmonary inflammation has long been believed to be crucial in the pathogenesis due to exposure to $PM_{2.5}$ (Rajagopalan et al. 2018). However, except for the time course studies (Brook et al. 2010), this notion has not been systemically investigated, primarily due to a lack of appropriate animal models. We previously induced pulmonary inflammation through lung epithelial cell-specific overexpression of constitutively active IKK2 using SPFTC-rtTA and tetO-cre alleles and demonstrated that pulmonary inflammation is sufficient to cause systemic insulin resistance (Chen et al. 2017). In the present study, this genetic manipulation strategy was exploited to delete endogenous IKK2 specifically in the lung epithelial cells. The lung epithelial cell–specific recombination of the IKK2 gene (Figures 1B–1D) and the lower number of DEP exposure–associated BALF immune cells and proinflammatory cytokines in KO vs. tgWT mice strongly support the suitability of these mice as a model system for studying the role of pulmonary inflammation in pathogenesis due to exposure to $PM_{2.5}$. The specified role of pulmonary IKK2 in the development of $PM_{2.5}$ exposure–induced pulmonary inflammation is consistent with the numerous previous studies that have shown that IKK2/NF-κB signaling pathway is central to the inflammatory response (Pahl 1999) and several other studies have implicated it in $PM_{2.5}$ exposure–induced pulmonary inflammation (Dagher et al. 2007; Kafoury and Madden 2005; Maciejczyk and Chen 2005; Mantecca et al. 2010; Nam et al. 2004). To the best of our knowledge, the present study is the first one to show the essential role of IKK2 in induction of pulmonary inflammation by exposure to DEP in living animals, thus providing a valuable animal model for the study of the pathogenic role of pulmonary inflammation in a complex process, such as the one due to exposure to DEP.

Both epidemiological (Alderete et al. 2017; Yang et al. 2018) and toxicological (Liu et al. 2017; Wang et al. 2018; Xu et al. 2017) studies have shown that exposure to $PM_{2.5}$ causes insulin resistance and glucose intolerance. Consistent with these studies, the present study reveals that long-term (e.g., 3- to 4-month) exposure to DEP resulted in marked insulin resistance and glucose intolerance in tgWT mice. In contrast, short-term (e.g., 2- to 3-month) exposure to DEP did not cause any significant differences in glucose homeostasis (Figures 3A–3D). This time dependency is consistent with recent epidemiological studies (Yitshak Sade et al. 2016). Notably, we previously showed that exposure to concentrated ambient $PM_{2.5}$ rapidly induced abnormalities in glucose homeostasis in diabetic KKAy mice (Liu et al. 2014). Taken together, these studies suggest that there may be populations who are potentially susceptible to $PM_{2.5}$ exposure, in particular individuals with increased risk for diabetes. Glucose tolerance is collectively determined by circulating insulin level and systemic sensitivity to insulin. The present study demonstrates that exposure to DEP resulted in lower systemic insulin sensitivity but greater glucose-induced insulin secretion in tgWT mice than are found in those exposed to PBS, suggesting that DEP exposure causes glucose intolerance primarily through induction of systemic insulin resistance. Furthermore, we show that DEP exposure was associated with lower insulin signaling in the liver but not in the adipose tissue or skeletal muscle. To our knowledge, the present study is the first one to assess the insulin sensitivity

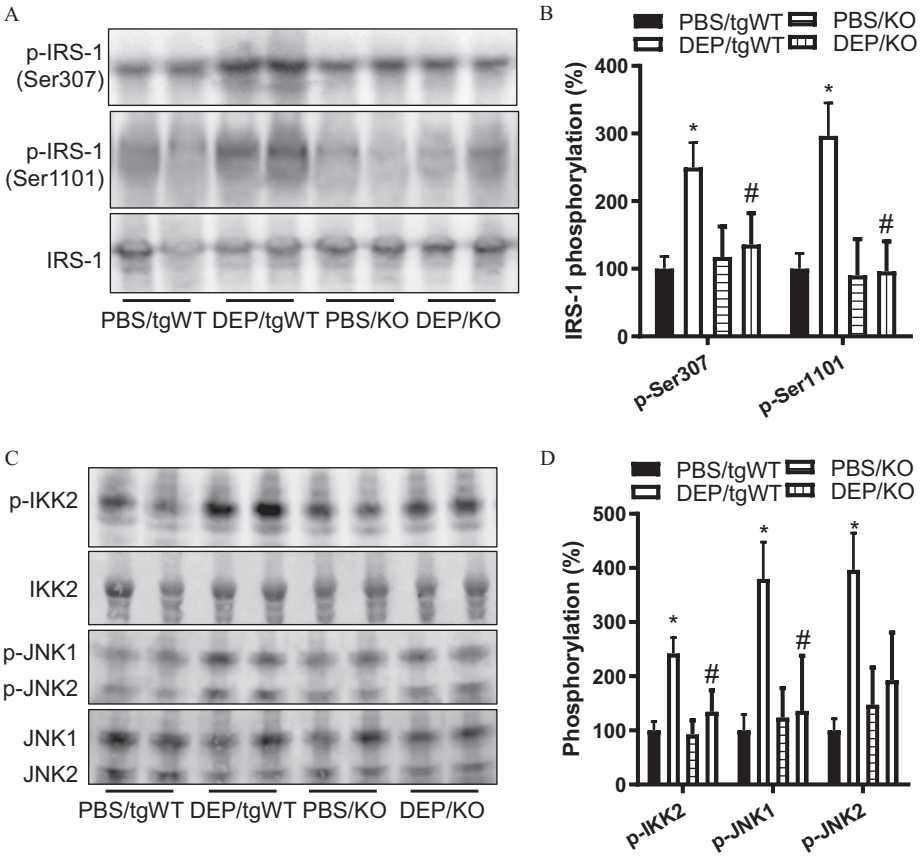

Figure 5. Hepatic IRS-1 phosphorylation and inflammatory response in diesel exhaust particulate matter (DEP)-exposed mice with lung epithelial cell-specific IKK2 deficiency. Western blotting analysis was used to determine hepatic IRS-1 Ser307 and Ser1101 phosphorylation levels (A and B) and hepatic IKK2 and JNK phosphorylation levels (C and D). The representative images (A and C) and quantitation data (B and D) are presented. To quantitate the phosphorylation, the phosphor-IRS-1, phosphor-IKK2, and phosphor-JNK levels was normalized to total IRS-1, IKK2, and JNK, respectively, and graphed in relation to phosphate buffered saline (PBS)/tgWT. $n = 6–8$/group. All data were expressed as means ± SEMs. $*p < 0.05$ vs. PBS, $^{\#}p < 0.05$ vs. tgWT, two-way ANOVA followed by Bonferroni correction.

effect of DEP exposure on all three insulin-dependent tissues simultaneously. The liver as the primary target organ for DEP exposure inducing systemic insulin resistance is consistent with our previous study (Liu et al. 2017), and lower hepatic insulin sensitivity after exposure to DEP is consistent with several previous studies by others (Jian et al. 2018; Xu et al. 2017; Zheng et al. 2013). However, it is noteworthy that we recently showed that, in a mouse model, exposure to concentrated ambient $PM_{2.5}$ promoted the inflammation of adipose tissues and decreased their insulin sensitivity (Hu et al. 2017). Therefore, further study is needed to verify the effect of $PM_{2.5}$ exposure on the insulin sensitivity of adipose tissues.

Another important finding in the present study is the demonstration that $PM_{2.5}$ exposure–induced hepatic insulin resistance was accompanied by hepatic inflammation, strongly supporting the hypothesis that the latter may play a crucial role in $PM_{2.5}$ exposure inducing hepatic insulin resistance. This finding was further supported by the DEP exposure–associated IRS-1 serine phosphorylation. These data are consistent with previous studies showing that exposure to concentrated ambient $PM_{2.5}$ (CAP) resulted in hepatic inflammation and IRS-1 phosphorylation at Ser1101 (Zheng et al. 2013). More important, the present study extended these findings, revealing markedly higher levels of IRS-1 Ser307 phosphorylation upon exposure to DEP in comparison with levels in mice treated with PBS. IRS-1 phosphorylation at either Ser1101 or Ser307 was shown to inhibit signaling transduction via the insulin receptor (IR) and thus to lead to insulin resistance (Copps and White 2012). Although IRS-1 Ser1101 was shown to be phosphorylated by protein kinase C-θ (PKCθ) and S6 kinase beta-1 (S6K1) in a setting of overnutrition (Tremblay et al. 2007), IRS-1 Ser307 was shown to be phosphorylated by JNK and IKK2 in response to TNFα treatment (Copps and White 2012). Therefore, phosphorylation of IRS-1 Ser307 is generally believed to be one of the molecular mechanisms for inflammation-induced insulin resistance. In line with the increased IRS-1 Ser307 phosphorylation, the present study demonstrates that DEP exposure was associated with significantly higher phosphorylation of JNK and IKK2, two central regulators of inflammatory responses. Collectively, these data suggest that DEP exposure–induced hepatic insulin resistance may result from a local inflammatory response.

As one of its primary goals, the present study has also provided deep insight into the pathogenesis of hepatic inflammation and consequent insulin resistance due to exposure to $PM_{2.5}$. The present data strongly suggest that egress from the pulmonary inflammatory response is central to the development of hepatic inflammation and insulin resistance due to exposure to $PM_{2.5}$. Evidence for this role of pulmonary inflammation include our finding that exposure to DEP was associated with significantly higher circulating proinflammatory cytokines, such as TNFα, and IL-6 in tgWT mice. These differences in circulating proinflammatory cytokines are consistent with findings in numerous previous studies (Bai and Sun 2016; Feng et al. 2016). Furthermore, we show that lung epithelial cell–specific IKK2 deficiency seemed to nearly abolish the higher circulating levels of proinflammatory

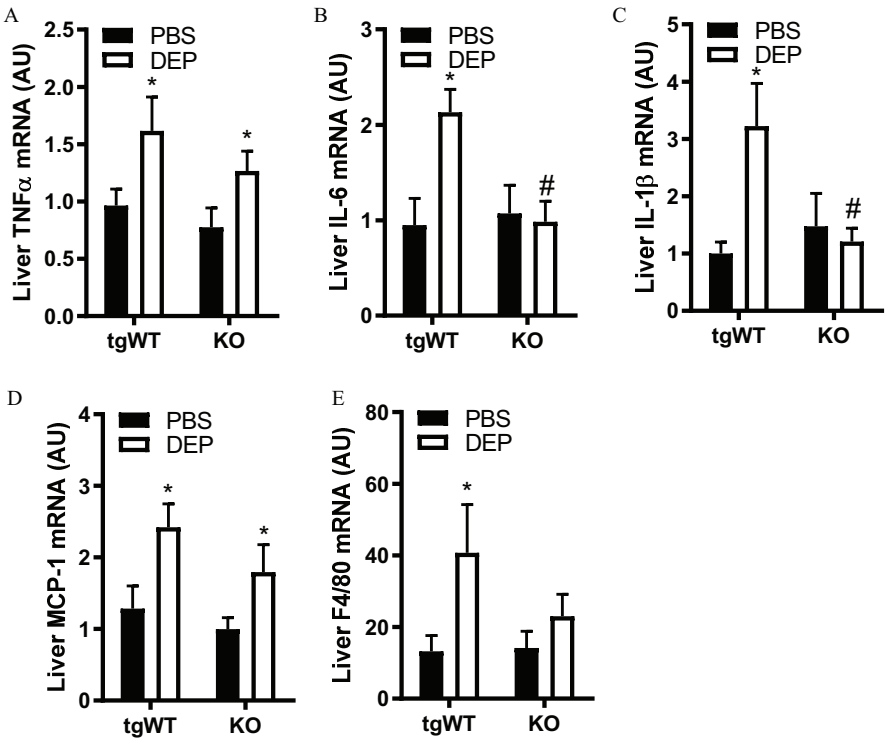

Figure 6. Hepatic proinflammatory cytokine expression levels in diesel exhaust particulate matter (DEP)-exposed mice with lung epithelial cell-specific IKK2 deficiency. Hepatic expression of the indicated inflammatory biomarkers was determined by real-time quantitative PCR (RT-PCR). $n = 6–8$/group. All data were expressed as means ± SEMs. $*p < 0.05$ vs. PBS, $^{\#}p < 0.05$ vs. tgWT, two-way ANOVA followed by Bonferroni correction. KO, SFTPC-rtTA$^{+/-}$ tetO-cre$^{+/-}$ IKK2$^{flox/flox}$ mice; tgWT, SFTPC-rtTA$^{+/-}$ tetO-cre$^{-/-}$ IKK2$^{flox/flox}$ littermates. PBS, phosphate buffered saline.

cytokines associated with DEP exposure, such that cytokine levels in DEP-treated mice were similar to those in PBS-treated mice (Figure 2).

Although additional work is needed to pinpoint its role, these findings suggest that in a transgenic mouse model, pulmonary inflammation is essential for the $PM_{2.5}$ exposure–induced increases in circulating proinflammatory cytokines. Given the well-established role of proinflammatory cytokines in various liver diseases, including inflammation and the demonstration of marked hepatic inflammation, it can be postulated that $PM_{2.5}$ exposure–induced hepatic inflammation may be subsequent to increased circulating proinflammatory cytokines, which in turn results from pulmonary inflammation. In contrast, the marked decrease in KO mice of DEP exposure–induced hepatic inflammation and insulin resistance almost rules out the possibility that extrapulmonary translocation of DEP components plays an important role in this pathogenesis, because no major metabolic change (reflected by BW assessment) was noted in KO mice.

Although the present study furthers our understanding of the mechanism of action of DEP, caution should be taken when extrapolating these results to ambient PM exposure due to the limitations of the present study. First, it should be noted that intratracheal instillation, although routinely used in toxicological investigations due to its multiple advantages, is different from actual human inhalation, particularly in the deposition pattern. This difference may influence not only the distribution of particles in the lung but also the exposure–response relationship (Osier et al. 1997; Silva et al. 2014). In addition, consistent with previous studies (Henderson et al. 1995; Robertson et al. 2012), the present results suggest a proinflammatory action of chronic instillation of PBS in the lung (Figure 1). Because all the experimental groups in this study were treated with PBS, this treatment is not expected to be a confounding factor in the study. However, further study is required to exclude the potential effect of this nonspecific inflammation on the sensitivity of mice to PM (Henderson et al. 1995). Moreover, although DEP may be the major source of ambient $PM_{2.5}$ in some areas, their chemical compositions are generally different. Therefore, further study is warranted to determine the role of pulmonary IKK2 in the development of glucose intolerance due to exposure to ambient $PM_{2.5}$. Another factor to note is that the KO mice had marked remaining IKK2 expression in the lung (Figures 1B–1D), which may be due to the presence of nonepithelial cells in the lung or the inefficiency of the cre system. In human lungs, only about one-third of total lung cells were epithelial cells (Crapo et al. 1982). Therefore, the presence of nonepithelial cells in the lungs was more likely the primary reason for the remaining IKK2 expression in the KO mice. Furthermore, the induced lung epithelial cell–specific knockout of IKK2 (Figures 1B-1D) was verified at the end of the 8-wk doxycycline feeding only. Because the mice were not fed the doxycycline diet beyond those 8 wk, we cannot rule out the possibility that the induced knockout of IKK2 was partly restored during the 4-month PBS/DEP instillation due to the turnover of lung epithelial cells.

Conclusion

Our findings suggest that in a transgenic mouse model, an IKK2-dependent pulmonary inflammatory response was essential for the development of abnormal glucose homeostasis due to exposure to DEP.

Acknowledgments

This work was supported by the National Institutes of Health (R01ES024516 to Z.Y.), the American Heart Association (13SDG17070131 to Z.Y.), the National Natural Science

Foundation of China (81500216 to C.M.), the 2016 Henan Province Health System Abroad Training Project (2016011 to S. C.), and 2017 Henan Medical Science and Technology Research Project (201702050 to S.C.).

References

Alderete TL, Habre R, Toledo-Corral CM, Berhane K, Chen Z, Lurmann FW, et al. 2017. Longitudinal associations between ambient air pollution with insulin sensitivity, β-cell function, and adiposity in Los Angeles Latino children. Diabetes 66(7):1789–1796, PMID: 28137791, https://doi.org/10.2337/db16-1416.

Bai Y, Sun Q. 2016. Fine particulate matter air pollution and atherosclerosis: mechanistic insights. Biochim Biophysic Acta 1860(12):2863–2868, PMID: 27156486, https://doi.org/10.1016/j.bbagen.2016.04.030.

Bide R, Yee E, Armour SJ. 1997. Estimation of human toxicity from animal inhalation toxicity data: 1. Minute volume-body weight relationships between animals and man. Medicine Hat, Alberta, Canada: Defence Research Establishment Suffield. https://www.researchgate.net/publication/277766604_Estimation_of_ 618 Human_Toxicity_From_Animal_Inhalation_Toxicity_Data_1_Minute_Volume-619 Body_Weight_Relationships_Between_Animals_And_Man [accessed 11 May 2019].

Bowe B, Xie Y, Li T, Yan Y, Xian H, Al-Aly Z. 2018. The 2016 global and national burden of diabetes mellitus attributable to $PM_{2.5}$ air pollution. Lancet Planet Health 2(7):e301–e312, PMID: 30074893, https://doi.org/10.1016/S2542-5196(18)30140-2.

Brook RD, Newby DE, Rajagopalan S. 2017. Air pollution and cardiometabolic disease: an update and call for clinical trials. Am J Hypertens 31(1):1–10, PMID: 28655143, https://doi.org/10.1093/ajh/hpx109.

Brook RD, Rajagopalan S, Pope CA 3rd, Brook JR, Bhatnagar A, Diez-Roux AV, et al. 2010. Particulate matter air pollution and cardiovascular disease: an update to the scientific statement from the American Heart Association. Circulation 121(21):2331–2378, PMID: 20458016, https://doi.org/10.1161/CIR.0b013e3181dbece1.

Chen M, Zhou H, Xu Y, Qiu L, Hu Z, Qin X, et al. 2017. From the cover: lung-specific overexpression of constitutively active IKK2 induces pulmonary and systemic inflammations but not hypothalamic inflammation and glucose intolerance. Toxicol Sci 160(1):4–14, PMID: 29036520, https://doi.org/10.1093/toxsci/kfx154.

Copps KD, White MF. 2012. Regulation of insulin sensitivity by serine/threonine phosphorylation of insulin receptor substrate proteins IRS1 and IRS2. Diabetologia 55(10):2565–2582, PMID: 22869320, https://doi.org/10.1007/s00125-012-2644-8.

Crapo JD, Barry BE, Gehr P, Bachofen M, Weibel ER. 1982. Cell number and cell characteristics of the normal human lung. Am Rev Respir Dis 126(2):332–337, PMID: 7103258, https://doi.org/10.1164/arrd.1982.126.2.332.

Dagher Z, Garçon G, Billet S, Verdin A, Ledoux F, Courcot D, et al. 2007. Role of nuclear factor-kappa B activation in the adverse effects induced by air pollution particulate matter (PM2.5) in human epithelial lung cells (L132) in culture. J Appl Toxicol 27(3):284–290, PMID: 17265450, https://doi.org/10.1002/jat.1211.

EPA (U.S. Environmental Protection Agency). 2018. Integrated science assessment (ISA) for particulate matter (external review draft). https://cfpub.epa.gov/ncea/isa/recordisplay.cfm?deid=341593 [accessed 2 December 2018].

Feng S, Gao D, Liao F, Zhou F, Wang X. 2016. The health effects of ambient PM2.5 and potential mechanisms. Ecotoxicol Environ Saf 128:67–74, PMID: 26896893, https://doi.org/10.1016/j.ecoenv.2016.01.030.

Guo S. 2014. Insulin signaling, resistance, and the metabolic syndrome: insights from mouse models into disease mechanisms. J Endocrinol 220(2):T1–T23, PMID: 24281010, https://doi.org/10.1530/JOE-13-0327.

Habre R, Zhou H, Eckel SP, Enebish T, Fruin S, Bastain T, et al. 2018. Short-term effects of airport-associated ultrafine particle exposure on lung function and inflammation in adults with asthma. Environ Int 118:48–59, PMID: 29800768, https://doi.org/10.1016/j.envint.2018.05.031.

Happo MS, Salonen RO, Hälinen AI, Jalava PI, Pennanen AS, Kosma VM, et al. 2007. Dose and time dependency of inflammatory responses in the mouse lung to urban air coarse, fine, and ultrafine particles from six European cities. Inhal Toxicol 19(3):227–246, PMID: 17365027, https://doi.org/10.1080/08958370601067897.

He M, Ichinose T, Yoshida S, Ito T, He C, Yoshida Y, et al. 2017. PM2.5-induced lung inflammation in mice: differences of inflammatory response in macrophages and type II alveolar cells. J Appl Toxicol 37(10):1203–1218, PMID: 28555929, https://doi.org/10.1002/jat.3482.

Henderson RF, Driscoll KE, Harkema JR, Lindenschmidt RC, Chang IY, Maples KR, et al. 1995. A comparison of the inflammatory response of the lung to inhaled versus instilled particles in F344 rats. Fundam Appl Toxicol 24(2):183–197, PMID: 7737430, https://doi.org/10.1006/faat.1995.1022.

Hu Z, Chen M, Zhou H, Tharakan A, Wang X, Qiu L, et al. 2017. Inactivation of TNF/LT locus alters mouse metabolic response to concentrated ambient $PM_{2.5}$. Toxicology 390:100–108, PMID: 28917655, https://doi.org/10.1016/j.tox.2017.09.009.

Jian T, Ding X, Wu Y, Ren B, Li W, Lv H, et al. 2018. Hepatoprotective effect of loquat leaf flavonoids in $PM_{2.5}$-induced non-alcoholic fatty liver disease via regulation of IRs-1/Akt and CYP2E1/JNK pathways. Int J Mol Sci 19(10), PMID: 30275422.

Kafoury RM, Madden MC. 2005. Diesel exhaust particles induce the over expression of tumor necrosis factor-alpha (TNF-alpha) gene in alveolar macrophages and failed to induce apoptosis through activation of nuclear factor-kappaB (NF-kappaB). Int J Environ Res Public Health 2(1):107–113, PMID: 16705808.

Kim YB, Peroni OD, Franke TF, Kahn BB. 2000. Divergent regulation of Akt1 and Akt2 isoforms in insulin target tissues of obese Zucker rats. Diabetes 49(5):847–856, PMID: 10905496, https://doi.org/10.2337/diabetes.49.5.847.

Kim YB, Zhu JS, Zierath JR, Shen HQ, Baron AD, Kahn BB. 1999. Glucosamine infusion in rats rapidly impairs insulin stimulation of phosphoinositide 3-kinase but does not alter activation of Akt/protein kinase B in skeletal muscle. Diabetes 48(2):310–320, PMID: 10334307, https://doi.org/10.2337/diabetes.48.2.310.

Kubesch NJ, de Nazelle A, Westerdahl D, Martinez D, Carrasco-Turigas G, Bouso L, et al. 2015. Respiratory and inflammatory responses to short-term exposure to traffic-related air pollution with and without moderate physical activity. Occup Environ Med 72(4):284–293, PMID: 25475111, https://doi.org/10.1136/oemed-2014-102106.

Kyjovska ZO, Jacobsen NR, Saber AT, Bengtson S, Jackson P, Wallin H, et al. 2015. DNA strand breaks, acute phase response and inflammation following pulmonary exposure by instillation to the diesel exhaust particle NIST1650b in mice. Mutagenesis 30(4):499–507, PMID: 25771385, https://doi.org/10.1093/mutage/gev009.

Li YJ, Shimizu T, Hirata Y, Inagaki H, Takizawa H, Azuma A, et al. 2013. EM, EM703 inhibit NF-kB activation induced by oxidative stress from diesel exhaust particle in human bronchial epithelial cells: importance in IL-8 transcription. Pulm Pharmacol Ther 26(3):318–324, PMID: 23291319, https://doi.org/10.1016/j.pupt.2012.12.010.

Liu C, Fonken LK, Wang A, Maiseyeu A, Bai Y, Wang TY, et al. 2014. Central IKKβ inhibition prevents air pollution mediated peripheral inflammation and exaggeration of type II diabetes. Part Fibre Toxicol 11:53, PMID: 25358444, https://doi.org/10.1186/s12989-014-0053-5.

Liu C, Xu X, Bai Y, Zhong J, Wang A, Sun L, et al. 2017. Particulate air pollution mediated effects on insulin resistance in mice are independent of CCR2. Part Fibre Toxicol 14(1):6, PMID: 28253935, https://doi.org/10.1186/s12989-017-0187-3.

Lucht SA, Hennig F, Matthiessen C, Ohlwein S, Icks A, Moebus S, et al. 2018. Air pollution and glucose metabolism: an analysis in non-diabetic participants of the Heinz Nixdorf Recall Study. Environ Health Perspect 126(4):047001, PMID: 29616776, https://doi.org/10.1289/EHP2561.

Lucht S, Hennig F, Moebus S, Führer-Sakel D, Herder C, Jöckel KH, et al. 2019. Air pollution and diabetes-related biomarkers in non-diabetic adults: a pathway to impaired glucose metabolism? Environ Int 124:370–392, PMID: 30660850, https://doi.org/10.1016/j.envint.2019.01.005.

Maciejczyk P, Chen LC. 2005. Effects of subchronic exposures to concentrated ambient particles (CAPS) in mice. VIII. Source-related daily variations in in vitro responses to CAPS. Inhal Toxicol 17(4-5):243–253, PMID: 15804942, https://doi.org/10.1080/08958370590912914.

Maeda S, Chang L, Li ZW, Luo JL, Leffert H, Karin M. 2003. IKKbeta is required for prevention of apoptosis mediated by cell-bound but not by circulating TNFalpha. Immunity 19(5):725–737, PMID: 14614859.

Mantecca P, Farina F, Moschini E, Gallinotti D, Gualtieri M, Rohr A, et al. 2010. Comparative acute lung inflammation induced by atmospheric PM and size-fractionated tire particles. Toxicol Lett 198(2):244–254, PMID: 20621170, https://doi.org/10.1016/j.toxlet.2010.07.002.

Nam HY, Choi BH, Lee JY, Lee SG, Kim YH, Lee KH, et al. 2004. The role of nitric oxide in the particulate matter (PM2.5)-induced NFkappaB activation in lung epithelial cells. Toxicol Lett 148(1-2):95–102, PMID: 15019093, https://doi.org/10.1016/j.toxlet.2003.12.007.

Osier M, Baggs RB, Oberdörster G. 1997. Intratracheal instillation versus intratracheal inhalation: influence of cytokines on inflammatory response. Environ Health Perspect 105 Suppl 5(Suppl 5):1265–1271, PMID: 9400736, https://doi.org/10.1289/ehp.97105s51265.

Pahl HL. 1999. Activators and target genes of Rel/NF-kappaB transcription factors. Oncogene 18(49):6853–6866, PMID: 10602461, https://doi.org/10.1038/sj.onc.1203239.

Rajagopalan S, Al-Kindi SG, Brook RD. 2018. Air pollution and cardiovascular disease: JACC state-of-the-art review. J Am Coll Cardiol 72(17):2054–2070, PMID: 30336830, https://doi.org/10.1016/j.jacc.2018.07.099.

Robertson S, Gray GA, Duffin R, McLean SG, Shaw CA, Hadoke PW, et al. 2012. Diesel exhaust particulate induces pulmonary and systemic inflammation in rats without impairing endothelial function ex vivo or in vivo. Part Fibre Toxicol 9(1):9, PMID: 22480168, https://doi.org/10.1186/1743-8977-9-9.

Silva RM, Doudrick K, Franzi LM, TeeSy C, Anderson DS, Wu Z, et al. 2014. Instillation versus inhalation of multiwalled carbon nanotubes: exposure-related health effects, clearance, and the role of particle characteristics. ACS Nano 8(9):8911–8931, PMID: 25144856, https://doi.org/10.1021/nn503887r.

Tremblay F, Brûlé S, Hee Um S, Li Y, Masuda K, Roden M, et al. 2007. Identification of IRS-1 SER-1101 as a target of S6K1 in nutrient- and obesity-induced insulin resistance. Proc Natl Acad Sci USA 104(35):14056–14061, PMID: 17709744, https://doi.org/10.1073/pnas.0706517104.

Wang W, Zhou J, Chen M, Huang X, Xie X, Li W, et al. 2018. Exposure to concentrated ambient $PM_{2.5}$ alters the composition of gut microbiota in a murine model. Part Fibre Toxicol 15(1):17, PMID: 29665823, https://doi.org/10.1186/s12989-018-0252-6.

Xu J, Zhang W, Lu Z, Zhang F, Ding W. 2017. Airborne $PM_{2.5}$-induced hepatic insulin resistance by Nrf2/JNK-mediated signaling pathway. Int J Environ Res Public Health 14(7):E787, PMID: 28708100, https://doi.org/10.3390/ijerph14070787.

Yang BY, Qian ZM, Li S, Chen G, Bloom MS, Elliott M, et al. 2018. Ambient air pollution in relation to diabetes and glucose-homoeostasis markers in China: a cross-sectional study with findings from the 33 Communities Chinese Health Study. Lancet Planet Health 2(2):e64–e73, PMID: 29615239, https://doi.org/10.1016/S2542-5196(18)30001-9.

Ying Z, Kampfrath T, Thurston G, Farrar B, Lippmann M, Wang A, et al. 2009. Ambient particulates alter vascular function through induction of reactive oxygen and nitrogen species. Toxicol Sci 111(1):80–88, PMID: 19182107, https://doi.org/10.1093/toxsci/kfp004.

Ying Z, Xie X, Bai Y, Chen M, Wang X, Zhang X, et al. 2015. Exposure to concentrated ambient particulate matter induces reversible increase of heart weight in spontaneously hypertensive rats. Part Fibre Toxicol 12:15, PMID: 26108756, https://doi.org/10.1186/s12989-015-0092-6.

Yitshak Sade M, Kloog I, Liberty IF, Schwartz J, Novack V. 2016. The association between air pollution exposure and glucose and lipids levels. J Clin Endocrinol Metab 101(6):2460–2467, PMID: 27218271, https://doi.org/10.1210/jc.2016-1378.

Zheng Z, Xu X, Zhang X, Wang A, Zhang C, Hüttemann M, et al. 2013. Exposure to ambient particulate matter induces a NASH-like phenotype and impairs hepatic glucose metabolism in an animal model. J Hepatol 58(1):148–154, PMID: 22902548, https://doi.org/10.1016/j.jhep.2012.08.009.